Chapter 5

Industrial Application of Synthetic Irradiance: Case study of solar yield

Miguel Larrañeta

Andalusian Association for Research and Industrial Cooperation (AICIA). Avenida de los descubrimientos s/n, 41092 Seville, Spain, e-mail:mlarraneta@gter.es

Carlos Fernández-Peruchena

National Renewable Energy Centre (CENER). C/ Isaac Newton 4, 41092, Seville, Spain, e-mail: cfernandez@cener.com

Manuel A. Silva Pérez

University of Seville. Department of Energy Engineering. Avenida de los descubrimientos s/n, 41092 Seville, Spain, e-mail: msilva@us.es

Abstract: Industrial activity concerned with the profitability and safety of investments can be supported and promoted by research through the creation of new mathematical modelling approaches, and the quantification and mitigation of uncertainties. In recent years there has been increasing interest in the adoption of probabilistic approaches to assess sources of uncertainty in solar energy systems to estimate their feasibility, considering yield estimates, investments, operation and maintenance costs, and solar resource. In this context, the synthetic solar irradiance data set approach emerges as a promising tool to emulate the variability inherent to the solar resource in confident designs and feasibility analyses of these systems. Chapter 5 deals with the requirements of the industry with respect to synthetic solar data, and how such requirements are currently addressed during the main stages of development of solar projects. We recap methods for benchmarking the success of generated synthetic irradiance, reviewing statistical indicators for that purpose. We discuss and compare the use of single annual and multiple synthetic annual data sets of solar irradiance in the first stages of solar projects, and present their uses in a case study application in a Concentrating Solar Power (CSP) plant with a similar configuration to a well-known operational Parabolic Trough (PT) plant located in Spain.

Keywords: Typical Meteorological Year, Plausible Meteorological Year, feasibility assessment, solar energy systems, solar yield, industrial applications

1 Introduction

At this stage in the book, the reader should be familiar with general principles of solar energy modelling, the objectives of synthetic generation of solar irradiance, and many of the current methods of generating them and validating them. The aim of this chapter is to give a brief overview of the historical evolution of synthetic generation, as well as its current concepts and industrial applications by using a case study and addressing the evaluation of a Concentrating Solar Power (CSP) plant energy yield. The reader will learn about the practical implementation of synthetically generated solar irradiance series, from series validation, to the advantages and strengths this scheme provides.

Flat-priced electricity feed-in-tariff, a set of payments for the electricity fed into the power grid produced by renewable energy, became a popular policy and was adopted by many countries. In this way, Small-scale developers (as home-owners) as well as medium to large-scale companies were encouraged to deploy renewable energies for the security of their investment's return [1]. Notwithstanding, even if feed-in-tariff has shown to be an effective policy mechanism [2], its application may lead to drawbacks in the promotion of renewable energies by means of digression rates, the period in which this policy is carried out, tariff prices, or the financial burdens facing by electricity consumers that in some cases are imposed by feed-in-tariff [3,4].

For example, Spain became a leader in solar energy in the first decade of the 21st century due to an attractive feed-in-tariff, growing very rapidly but unsustainably; subsidies were drastically reduced by the Spanish government due to the 2008 financial crisis (from 3.1 GW installed in 2008 to only 500 MW per year). Spain, as well as other European countries, moved from a feed-in-tariff frame to an auction system in line with the Commission’s recommendations between 2014 and 2016. In this scenario, for current projects with variable prices, understanding the temporal distribution and variabilities of solar irradiation may be critical for its viability, due to the sensitivity of electricity systems to climate and weather variability [5]. The

variability of both renewable energies production and demand leads to periods in which the demand is not met (positive residual load), as well as periods with renewable surplus generation (negative residual load) [6], that hinder the sought goal of balancing supply and demand over high (less than seconds), medium (minutes to days) and low (month to years) time scales.

Different stages of a project's development require varying degrees of detail in the description of the variability of the resource. For example, for site selection, it would be enough to assess the temporal variability of the electricity production throughout the year, as well as during typical daily cycles, in order to compare potential yields among alternative sites. Nonetheless, once a specific site has been determined to be feasible for a solar power project, more precise and detailed solar irradiance data sets are required for its techno-economic optimization, which should take into account utility tariff structures, plant initial investments, incentives, financial structures, and annual costs from the achievement of proper plant operations (operation and maintenance costs). For this optimization, it is useful to calculate a full multi-year cash flow with some economic metrics, such as the Levelized Electricity Cost ('LEC') (also known as or the Levelized Cost Of Electricity, or 'LCOE') [7]. The LEC can be defined as the value that would have to be assigned to every unit of energy produced by a power plant throughout a determined period in order to equal the total costs incurred during this period as expressed in currency.

In this regard, characterizing the available solar resource of a region or at a specific location is key for energy policy decisions, engineering designs, and considerations of deploying solar energy systems. At this point, it is worth mentioning the 'Climate Normals' [8], as a representation of the long term values of solar irradiation and meteorological variables, defined with the intention of allowing comparison among observations from around the world. Initially, a 30-year period of reference was established as representative of the long term (mainly because, when the recommendation was first made, 30 years of good quality measurements were available for summarization), even if currently 15-year or 10-year periods are used at several meteorological institutes for calculating Climate Normals. The most used periods for Climate Normals are 1901-1930, 1931-1960 and 1961-1990. The strict definition of the time spans used for climate normals enables them to be used as references to which current data can be compared.

Unfortunately, average values provides an incomplete description of the climate, and they do not meet the needs of engineering design, which requires a deeper description on frequency distribution and statistical behavior, such as the variability at different time scales, extreme values, or the frequency of extended periods when a value is above a threshold. In addition, for renewable energy projects, it is worth highlighting the interdependency of meteorological variables. Even if solar radiation is primarily driven by astronomical and geographical parameters, it influences the atmospheric temperature, which in turn controls wind dynamics and cloud formation, which finally affects solar radiation [5]. The co-variability of solar radiation, wind velocity and temperature, has a twofold implication: they rule the balance between solar, wind-power and energy demand [9], and also affect the electricity generation technologies themselves. For example, wind induces heliostat tracking errors, the deformation of parabolic trough collector structures affects their optical performance [10], and temperature (as well as cooling effect of wind) affects the photovoltaic modules performance [11].

Solar irradiance modeling provides a metric of the power availability from the sun over a given time period, which is required in a wide range of applications, including assessments of a location in the planning phase of a solar energy system, forecasting the power that is available for solar energy plants to compete in electricity markets, estimating the energy demands of a property, assessing crop yields, providing ultraviolet exposure data for public health interests, and, importantly, in estimating the grid impacts from increasing penetrations of PV into an electricity network [12]. Among the different uses of solar irradiance modelling forecasting, elaborations of historic data sets, and synthetic generation merit special attention.

Forecasting allows us to predict future solar irradiance based on given conditions as framework and typically ranges from a few minutes to several days ahead ([13–16]). Historical data sets allow a long-term assessment of the solar resource; they are typically used for statistical information for projections into the future [17,18]. ‘Synthetic generation’ is a term that denotes bringing together a variety of models to generate statistically accurate time series when real data sets are unavailable, to fill in gaps in data sets, or to increase the temporal resolution of a data set [12].

Unlike the solar position, which is entirely regular, solar irradiance is influenced mostly by cloud cover, which, though determinable in principle, eludes modelling to the extent that it is effectively stochastic [19]). The degree of intermittency of

solar irradiance depends mainly upon the temporal scale with which it is observed [20]. ‘Ramping events’ (that is, steep transients) occur in inverse proportion to the durations of time used for scaling (Lave, et al. 2012). These events are caused by clouds, which affect solar irradiance on time scales measured in mere minutes. It is noteworthy that atmospheric aerosols also influence solar irradiance’s variability, but their effects are relevant only on time scales of several hours [21].

A few years ago, the solar industry recognized that the hourly time frequency (typically used) was not sufficient to simulate transient processes in power plants, which may have some influence on energy yields, and a higher time resolution was recommended for due diligence [22]. In this way, simulations model at higher frequencies than 1h provided realistic estimates of electrical production, especially when they coincide with partial cloud cover [23]. This led to the adaptation of the Heliosat scheme to use of 15 min solar irradiance time series derived from Meteosat Second Generation (MSG) satellite [24], as well as to the development of methodologies for increasing the temporal resolution of solar radiation series [25–28].

The impact of these potentially challenging transient effects occurring at a high frequency must be taken into account in CSP technology evaluation studies through dynamic models for which high temporal resolution solar irradiance (global for conventional PV, DNI for concentrating systems) data are required as input [29]. As an example, changes in the production of CSP plants caused by transient cloud effects can exceed 50% of the generation potential in the absence of clouds over 2 to 5 min [30]. Rapid changes in solar irradiance affect the integration of solar power in the energy mix, as the power output’s variability impacts the power systems’ reserve requirements, net load variability, regulation requirements, and the operations of other generators [31]. To illustrate this, Fig. 1 (bottom) shows the estimated production of a parabolic trough plant of 50 MW nominal power, and 7.5 full-load thermal storage system equivalent hours when running simulations with a one-minute observed DNI data (left), and their average hourly values (right). It can be observed that the cloud transients are markedly smoothed when integrating the one-minute data to an hourly resolution, which implies an overestimation of the power produced. The daily gross power produced at one-minute resolution is 392 MWh while at hourly resolution is 455 MWh, meaning a difference of more than 15 percent because of the input data time resolution.

Fig. 1 DNI (top) and estimated gross production (bottom) of a 50 MW nominal power parabolic trough plant at one-minute (left) and 1h (right) temporal resolutions on 15th June, 2016.

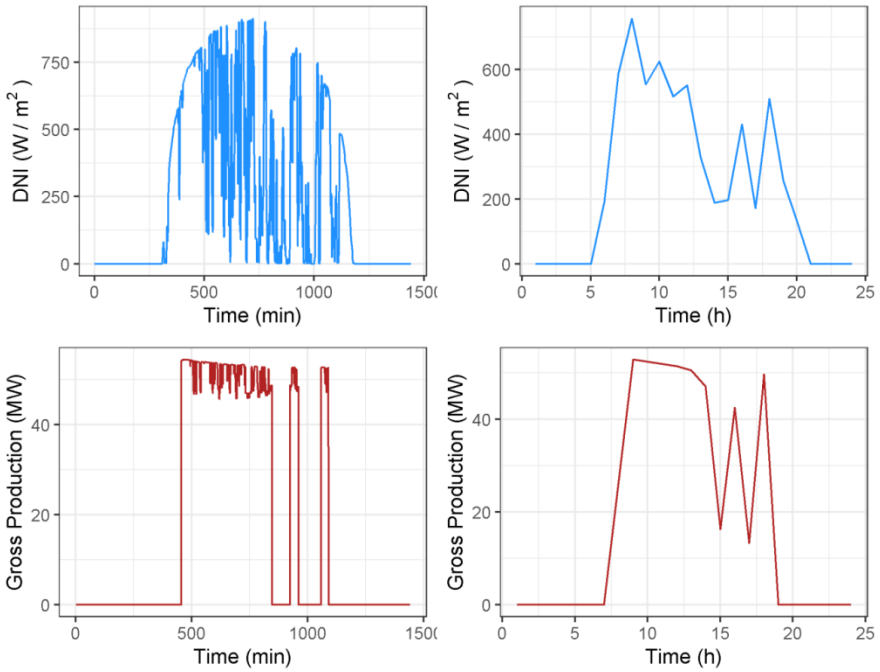

Instead of using a limited number of yearly data sets for simulation, the use of Monte Carlo methodologies to generate an unlimited number of yearly series is proposed by Nielsen, et al. [32]. This methodology allows the solar resource assessment - and thus the energy output calculation - to be performed in a similar way as that which is currently used for estimating other essential variables in economic assessments of solar power plants. The generation of hundreds of such plausible meteorological years has been demonstrated by Fernández-Peruchena, et al. [33] and Meybodi, et al. [34]. Other authors found issues with the Monte Carlo approach and suggest the Latin hypercube sampling method [35,36].

Section 2 of this chapter outlines industrial applications of synthetic solar irradiance time series such as CSP yield and building energy performance assessments, as well as a brief historical overview on the solar resource, starting from the proposal of initial assessment products (consisting on specific days or a single meteorological year) to their evolution to synthetic solar irradiance time series (consisting on synthetically generated meteorological years at a high frequency).. In Section 3, a case study of the application of synthetically generated meteorological years is shown through the estimates of the energy yields of a CSP plant compared. Section 4 constitutes the Summary and Conclusions, which are followed by our acknowledgements.

2 Industrial applications of synthetic time series

This section briefly outlines a historical perspective of solar resource assessments, from initial proposals based upon short representative periods to their evolution up to the proposal of the generation of synthetic years, as well as discusses some key industrial applications of synthetic solar irradiance time series.

To design and simulate solar energy collection systems, a first approach relies on the definition of its performance and economics under normal operating conditions, from which the optimization of the system is sought (taking into account conditions related to the costs of the technology and technical specifications, among other conditions). Since the operation of solar energy systems is variable, time series of solar irradiance and meteorological variables were suggested for representing normal operating conditions in systems simulation. From the pioneering work of Benseman and Cook proposing one of the first meteorological data sets for simulations [37] based exclusively on solar radiation, a number of procedures have been developed. Some of them are based on the definition of 'representative' days, or on periods of less than one year, i.e., 'short reference years', or SRY [38–40], but most of them rely on the use of an entire year [41–43] through the concatenation of twelve real months from available historical databases, or, less often, the selection of a most representative year [44]. Among these methods, the Test Reference Year (TRY) [45] and, specially, the Typical Meteorological Year (TMY) stood out in its wide application [46].

The TRY methodology takes into account GHI, ambient temperature and daily maximum ambient temperatures for the selection of the most twelve representative months (from January to December), based on the proximity of their mean values and standard deviations to corresponding long term values. TRY becomes Design Reference Year (DRY) when adding some new variables (such as five-minute DNI values), and forecast information [47]. TMY methodology takes into account GHI, maximums, averages, minimum air temperatures and levels of relative humidity, and maximum wind speeds, and computes the weighted sum of the Finkelstein-Schäfer (FS) statistic [48] to select five candidate months between January and December, which are ranked according to the closeness of a given month to its

actual long-term mean and median. TMY reproduces meteorological natural daily and seasonal variations and represents a year of typical climatic conditions for a given location. Even though the TMY was originally designed to meet requirements for building heating and cooling load calculations, it has been also widely used by solar-energy project developers as inputs for energy yield simulation of solar energy conversion system (such as System Advisor Model, PVSYST, or PVWatts), designing and sizing, as well as for comparing the expected performance of a proposed solar power plant at alternative sites. From its initial conception, applied to twenty-six sites in the United States, the next TMY version (TMY2) was carried out to respond to the demand for more locations (239 sites, for the period between 1961 and1990) [49], and subsequently refined and extended to 1,020 sites (TMY3, representative of the period 1991-2005) [50].

Over the years, modifications of TMYs have been proposed by several researchers [32], though it should be noted that the initial procedure has not been substantially modified. From a methodological point of view, the main differences presented in these methodologies are related to the variables required to build the final meteorological series, their weighting factors, the source of data (measured and/or modelled), or the application of different criteria in the final selection of the month from the candidate months [51]. Among these, it is worth mentioning data sets designed for evaluations of specific solar conversion technologies, as is the case of typical global year (TGY) and the typical direct year (TDY) for photovoltaics and concentrating solar power, respectively [52], as well as the typical solar year (TSY) [53], oriented to the bankability analysis of solar energy projects. However, some inconsistencies in TMY weather files have been noted which are attributed to the methods applied to their elaboration and/or the length of historical data used in constructing the files [54].

Despite its widespread use, TMY has raised many questions in recent years, and its suitability for solar projects is under debate. One of the main limitations of this approach stems from the fact that a single “representative” year actually corresponds to a “frozen state”, where the system description stands unchanged for different project horizons. This has implications in the techno-economic description of a solar based project. As investments in solar projects grow, the need for risk mitigation through more accurate descriptions and designs also grows. In particular,

in order to evaluate the likelihood of achieving the economic return of the investment and the associated risk of capital-intensive energy projects (such as CSP ones), the assessment of the CAPEX (the facility investment cost) and the OPEX (Operating Expenditures during the facility lifetime) are often required [55]. These techno-economic parameters take into account both system performances and economic factors for estimating costs and revenues over the lifetime of a project. It is worth mentioning that the lifetime of solar energy systems can have a long duration, from design to construction and commissioning, as well as operations and the final decommissioning. Typical timespans are 25-30 years for PV and CSP solar plants, and from 10 to 50 years for distributed energy resource projects [56]. Traditionally, CAPEX and OPEX have been described with a deterministic scheme:

- The plant yield obtained by the energy model is calculated by means of a TMY, which corresponds to a single point that is representative of long-term conditions.
- Input data to feed the financial model (the rate of inflation, weighted average capital costs, etc.) are point values, which allow to estimate financial performance parameters of the investment project (such as LEC).

As a consequence, for solar project plants, a given set of inputs used to feed the models always yields the same set of output values. Furthermore, the analysis of uncertainty and risk for solar projects' success is being increasingly recognized [32,57], especially for capital intensive ones [58]. It is worth mentioning that uncertainties can be divided into aleatory uncertainty (random), and epistemic uncertainty (limited knowledge):

- Aleatory uncertainty is due to natural variation of the system under investigation [59], and is treated in a probabilistic framework. It is also known as variable, irreducible, stochastic, or type A uncertainty.
- Epistemic uncertainty stems from a lack of knowledge, and may be specified in a probabilistic or non-probabilistic way, including second-order probability, interval, evidence theory, and fuzzy sets [60,61]. It is also known as state of knowledge, reducible, subjective, or type B uncertainty.

Within this deterministic scheme, a project's risk is evaluated through a sensitivity analysis carried out by varying the different parameters that compose

both the CAPEX and OPEX of an investment, which are related to the technical design and operating parameters of the project and ultimately affects system performance. These parameters are variable within a range depending on their uncertainties, from which the effects of the outputs of the financial model are analyzed [62].

Unfortunately, this traditional sensitivity analysis is not appropriate for risk assessments, as it lacks an explicit probabilistic measure of risk exposure. Confidence and uncertainty associated with the results are unknown (i.e., it doesn't contain an explicit quantification of the likelihoods of the different scenarios that might happen, stated in Type A uncertainties [63]). Consequently, there is a need to provide a probabilistic description for profitability assessments and annual paybacks. In addition to the most probable scenario provided by TMY annual series, information related to the project annual payback in a bad year is usually required by the developers and lenders [64].

Because of these reasons, TMY, though extensively used for feasibility studies of solar projects, is not well-suited to assess associated risks in the design, construction, and operation of solar projects regarding their natural variations. In particular, as a TMY represents typical rather than extreme conditions, it is not suitable for detailed designs of solar energy systems that have to handle worst-case conditions at a given location.

To address these uncertainties in the solar resource in a TMY scheme, the currently most-common approach relies on the use of time series representing an adverse scenario, corresponding to a year where the annual solar irradiation is expected to be exceeded by a high percentage of the years during the power plant's lifetime, which is usually called PoEXX (Probability of Excedance of XX%) or simply PXX [62]. In solar energy projects the solar resource assessment is frequently based both on the mean (PoE50) and extreme (PoE90, PoE99) years. Likewise, other probabilities of exceedance (e.g., PoE75) of the annual energy output are also required by promoters. The annual probability of exceedance is the probability that a given annual cumulative value of solar irradiance will be exceeded in any year. Given a random variable X with continuous and monotonic probability density function $f(x)$, a quantile function $Q_{f,}$ assigns to each probability p attained

by *f*, the value *x*, for which $P_r(X \leq x) = p$. The quantile function can be represented as follows:

$$Q(p) = F^{-1}(p) = \inf\{x; F(x) \geq p\}, 0 < p < 1.$$

Quantiles are points in a distribution that relate to the rank order of values in a given distribution, where the percentiles (P) are the description of quantiles relative to 100. In this way, the 90th percentile is 90% of the way up an ascending list of sorted values of a sample, and the 50th percentile (or median) is halfway up this rank order.

The probability of exceedance is complementary to the percentile. For example, a PoE75 corresponds to a P25. In Figure 2 we present a Weibull distribution for fifteen annual DNI values for the city of Seville, Spain, with PoE50 and PoE75 annual values.

Fig 2. Weibull distribution for fifteen annual DNI values for the city of Seville, Spain

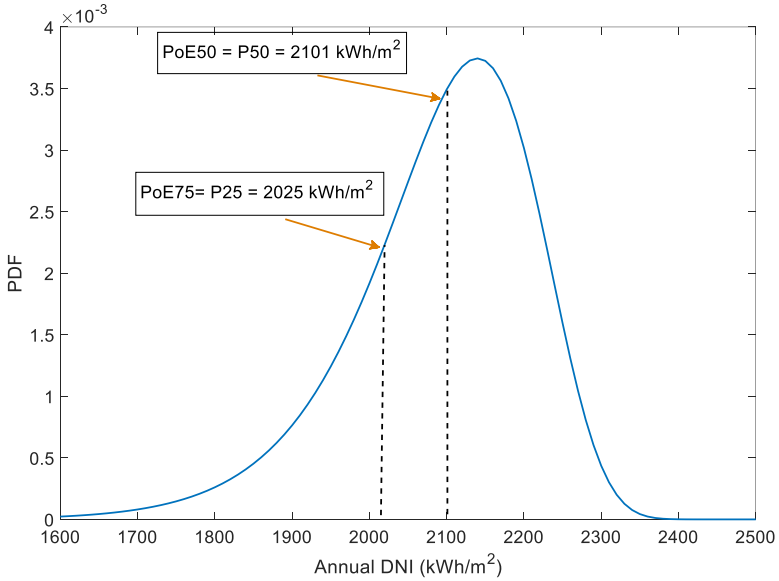

It has, however, been demonstrated that annual solar irradiation values are not uniquely related to net energy yield of solar plants, which implies that it is not sufficient to provide only the PoE90 DNI value. A PoE90 meteorological year is

required to simulate the plant's energy output from a meteorological series [64,65]. In recent years, different methodologies have been proposed, both for generating PoE90 annual series [66,67], and for any PoEXX annual series [53,65]. Even if most of these proposals have a methodological path similar to a TMY methodology (based upon a selection of months in a given year), no consensus has been established either on the generation of these series, or on a selection of monthly irradiation values. Nonetheless, it is noteworthy that there exist standardized procedures at national level [68].

Aside from the aforementioned techniques, a paradigm shift exists that proposes the adoption of probabilistic approaches to model the variability and uncertainties inherent to solar energy systems. This paradigm is motivated by the increasing importance of technical and economic evaluations of solar harnessing systems for industry and research, and it relies on the fact that the reliability of results depends upon assumptions about parameters. For example, a reduction of evaluations of solar energy systems to a single, deterministic figure (e.g., levelized cost of electricity (LCOE) for solar power plants) may lead to inaccurate results [69].

Probabilistic approaches can more accurately assess systems and scenarios, and, consequently, achieve more sound estimates of the economic feasibility of a given solar energy system [33,35,64,69,70]. Within this scheme, the economic feasibility addresses the variability of the solar resource, the cost of key investment and operation and maintenance elements, and the uncertainty associated with the performance and costs models [10]. This scheme relies upon probabilistic tools that, through uncertainty analyses, are able to describe the impacts of system uncertainties upon simulated performance metrics.

Such probabilistic methods assess the likelihoods of the simulated metric's probability of lying above or below a particular value, or within a specific range [35], and facilitate the evaluation of systems and scenarios through the assessment of the system performance and the main factors affecting it [69]. As an example, the Hybrid Optimization of Multiple Energy Resources (more commonly referred to by its acronym, 'HOMER') Pro software provides a multi-year module" that is designed to model distributed generation and microgrids [71]. This module allows modelling the changes that can occur over the course of a project as a function of

degradation in the performance of some components, demand changes, fluctuations of operational costs, etc. These changes are expressed in terms of yearly percentages, or, alternatively, by year-to-year series of multipliers matched to forecasts [72]:

- Grid price. The impact of utility price escalation during a project's lifetime is a key factor for accurately modeling and comparing the financial benefits of different distributed energy investments.
- PV degradation. The long-term performance of solar modules is externally influenced by temperature, snow, dust, precipitation, and humidity. At the array level, it is worth mentioning, also, module mismatches and shading effects. All of these factors result in different mechanisms of degradation that lead to stress during a PV system's lifetime.
- Battery degradation. This occurs from both charge-discharge cycles (calendar life), and cyclic charging and discharging (cycle life) [73]. Assessing these mechanisms is essential for envisaging the battery lifetime during system operations.
- Diesel price fluctuations. Significant variations in diesel prices may occur from different factors. Such fluctuations have drawn attention to the utilization of renewable energy sources towards the stabilization of overall energy prices [74].
- Load growth. During projects' lifetimes, both load demand increments and decrements may occur, and their effects on system performances must be considered.

The methods for the synthetic generation of PMYs usually rely on the use of the whole available series provided by satellite images or numerical weather prediction models, typically more than 10 years. By using the original series, the system design can take into account the observed variability of the solar resource at the site, assuming that future trends may be characterized by past trends. However, this approach is limited to the number of years available in the database, whereas the PMY synthetic generation model emerges as a promising tool that enables the stochastic simulation of solar harnessing systems that consider the uncertainty and variability inherent to the solar resource.

Synthetically generated solar irradiance series are designed to ensure that the full range of possible conditions are evaluated [75], based on the analysis of solar irradiance at different temporal scales [27,70,76–80]. The annual series synthetically generated with this purpose have been defined as Plausible Meteorological Year (PMY), as opposed to the TMY. Specifically, PMYs are defined as a high-frequency yearly series of GHI, DNI and other relevant meteorological variables (temperature, relative humidity, wind speed), which are consistent with corresponding monthly and annual series at a site, thus preserving natural variability characteristics [33].

Within the PMY scheme, input parameters related to solar energy systems and performance and economics parameters should be treated as probability distributions, not as specific values, that honor the inherent uncertainty in many of the system features and processes [36]. A solar project development requires simulation to assess technical risks and optimize plant layout. The simulation from a sufficiently large number of PMYs ensures the detailed probabilistic description of the system performance, and thus provides additional and valuable information for the project finance phase, leading to a better estimation and understanding of the uncertainty and potentially lowering the financing costs.

The development of PMYs was initially oriented to CSP projects, but the concept is applicable to other projects based on renewable energy technologies, especially for large solar energy installations. One of the most crucial phases of these projects is, undoubtedly, project finance. In this phase, a prognosis of expected energy yields, and corresponding economic incomes of the plant, is a necessary step. This requires not only the use of accurate simulation software, but also a reliable estimation of the solar resource in the location where the plant will be built, since solar resource assessment is one of the main contributors to the uncertainty of the energy yield assessment. In project finance, the interest rate depends significantly on the financial risk of a project and, therefore, limiting or correctly assessing the uncertainty of the solar resource and energy yield estimations is a direct means of lowering project finance costs.

At the same time, the appropriateness of using a TMY in assessing building energy performance has long been discussed, primarily since they don’t provide

enough information on plausible weather conditions as well as their probabilities [81]. As a consequence, the energy consumption assessed through TMY data does not necessarily represent the average values calculated on the historical meteorological years that it represents, as demonstrated by Hong, et al., [82] through the comparison of weather impacts using thirty years of historical data against TMY files in different types of office buildings with different design efficiencies in all ASHRAE climate zones. The following methods are currently used to take into account variations of historical weather data in building energy analyses as TMY alternatives:

- To use several data types (typical, cold and hot weather) so that weather variations are included in the analyses [83].
- To use all recent weather data to assess long-term weather variations according to their likelihood [84]. This approach has been used to investigate the impacts of weather variability and uncertainties on sizing HVAC (Heating, Ventilation, and Air Conditioning) systems [85].
- To generate synthetic weather conditions. A stochastic model based on a Vector Auto-Regressive process based on a historical weather data set was proposed for this purpose [57].

In this context, building energy assessment through PMYs provides new insights in the so-called forward uncertainty analysis (also called uncertainty propagation): the probabilistic modeling approach through PMYs ensures that a wide spectrum of potentially demanding conditions are evaluated, facilitating for example the quantification of the energy use or carbon emissions using building energy models with input variations [86]. Key benefits in this area stem from the fact that (in addition to meteorological conditions) the factors influencing energy use in buildings such as occupant behavior or thermal properties of building envelope are inherently uncertain [87,88]. Other benefits of this approach include the accurate evaluation of predictions performance, concept specific design guidance, testing the robustness of the design under variations in operational scenarios, and ultimately sizing systems according to realistic load variations over the buildings lifetime (instead of applying a generic safety factor). In this case, the system parameters can be perturbed assuming a certain distribution and used for sampling, and different densely occupied scenarios can be defined as discrete sets, weighted-based on

likelihood of occurrence and sampled [89]. Finally, it is worth mentioning efforts in evaluating the impact of climate change in buildings, as well as the subsequent adaptation of buildings to new scenarios [90,91].

3 Case study: Long-term yield assessment for a CSP plant in Spain

The assessment of the long-term energy yield of medium and large size solar energy plants is required from the earliest stages of solar energy projects. While in the pre-feasibility stage, such assessments can be based on the average monthly or yearly values of the relevant variable (GHI for PV, DNI for CSP), more detailed information is required in later project phases. Ideally, this information would consist of a time series of hourly or often sub-hourly values of solar radiation and other meteorological variables measured at the project's location over the course of multiple years. Unfortunately, there are few locations where such information is already available. In this case, a common practice is to use synthetic series, such as the TMY, PoEXX and PMY series as described in Section 2.

Current practice is to use a TMY for long-term yield estimations in feasibility analyses, complementing them with one or two PoE series (PoE75, PoE90, PoE99) for a financial risk analysis. While the TMY ideally represents the average solar resource during a project's lifetime, the PoE series corresponds to unfavorable scenarios in terms of the extant solar resource and, consequently, for the project's energy yields and economic returns. Both TMY and PoE series may be derived from any available ground measurements, or from modelled data.

A recent approach is to use a large number of PMYs, which are synthetically generated yearly series that are consistent with the observed statistical characteristics of the solar resource at the project location, allowing for a stochastic assessment of the energy yield. This is usually referred to as a 'multiyear approach'.

In this Section, we exemplify and compare both TMY and PMY approaches by applying them to the long-term yield assessment of a hypothetical CSP plant located in Sevilla, Spain.

The radiometric variable of interest for CSP systems is the direct normal irradiance, or DNI. Thus, the solar resource information consists of:

- Fifteen years of one-minute values of DNI;
- three single-year hourly series (TMY, PoE90, PoE99) constructed from the data, and
- 100 years of synthetically generated annual time series of hourly DNI, as determined by the statistical characteristics of the measured DNI data.

The characteristics of the CSP plant used for this example are similar to those of Andasol 3 [92], a commercial CSP plant with a relatively large thermal energy storage (7.5 hours of full-load capacity) located in the south of Spain. The main characteristics of the modelled plant are summarised in Table 1.

Table 1 Main characteristics of the Andasol 3 solar plant [92]

Net output at design (MWe)	50
Collector	EuroTrough ET150
Receiver	Schott PTR70 2008
Number of loops (4 collectors per loop)	156
Solar field aperture area (m2)	510,120
Heat Transfer Fluid	Therminol VP-1
Design loop/receiver inlet/ outlet temperature (ºC)	293/391
Thermal Energy Storage capacity (full-load equivalent hours)	7.5

3.1 Observation data sets

We have used one-minute average values of DNI recorded during fifteen consecutive years (2002–2016) in Seville, Spain. The measurements were taken with a sampling frequency of 0.2 Hz. A first-class Eppley NIP pyrheliometer mounted on a sun tracker Kipp & Zonen 2AP measures the DNI. The devices are located at the meteorological station of the Group of Thermodynamics and Renewable Energy (GTER) at the University of Seville. The geographical coordinates of the station are shown in Table 2.

The quality and integrity of the data is essential to guarantee reliability and trustworthiness of the yield estimates. In the case of measured data, the quality of the sensors and data acquisition system, the maintenance procedures of the

measurement station and the quality control procedures, including, if necessary, the gap filling techniques used, should be properly documented. An incorrectly maintained station or lack of care in data processing may result in unreliable data that, in turn, will lead to incorrect yield estimates.

Thus, the GTER station is subject to a maintenance and calibration procedure in accordance with the recommendations of the instruments' manufacturers, including periodical calibrations of the solar radiation sensors. In addition, a quality control procedure is systematically applied to the data. This procedure is based on the recommendations of Baseline Solar Radiation Network (BSRN) [93], complemented with the detection of missing or incorrect data (gaps) and the application of gap-filling techniques to complete the series, if necessary. For the interested reader, a complete description of these procedures can be found in [94]. This specific data is not publically available at time of writing. Discussion surrounding measurement instrument uncertainty was covered in Chapter 4.

Table 2 Geographical coordinates of the GTER station, climate of Seville and period of measurements used for this analysis.

Classes	Latitude (°N)	Longitude (°W)	Altitude (m)	Climate	Period
Seville	37.4	6.0	12	Mediterranean	2002-2016

3.2 Solar resource characterization by means of single-year synthetic data sets

Simulation tools used for the yield assessment of solar plants typically require a single annual set of meteorological data representative of long term average conditions, defined as a typical meteorological year (TMY) [46]. Accordingly, their results represent expected average yield values.

There are several methods for generating TMYs based on long-term series of solar radiation and other meteorological variables. Current methods usually rely on the use of time series that typically provide 10-20 years of good quality ground measurements or satellite-derived data at hourly or sub-hourly resolutions. Although ground measurements from a station at the project site or from a nearby location are preferred, there are very few locations where such information is

available. In this case, solar radiation site-adapted estimates from satellite images can be used [95,96]. The procedure commonly consists of the following steps:

- Calculating the monthly cumulative values for all months included in the time series.
- For each month of the year, select the most representative month of the series from any of the years. The selection criteria depend on the application, and differs by method. The simplest methods are based on the selection of the month with the cumulative value of the relevant variable (DNI for CSP, GHI for PV) closest to the average for that month. Other, more sophisticated methods assign different weights to each variable to calculate a statistical indicator whose value is used as a criterion.
- Once the representative months for each month of a year have been selected, the data sets corresponding to the selected months are concatenated. The procedure might allow for changes or substitutions to produce monthly target values (see, for example [97]).

In our case study, we use fifteen years of one-minute measurements. The TMY has been constructed by the UNE 206011:2014 procedure [68]. In Figure 4, we present monthly observed values in a box plot with the TMY.

Fig 4. Box plot of the observed monthly values with TMY for Seville, Spain. Each box indicates the values comprised of the 25th (P25) through the 75th (P75) percentiles. Red horizontal lines indicate medians, and black horizontal lines represent the extreme observed values.

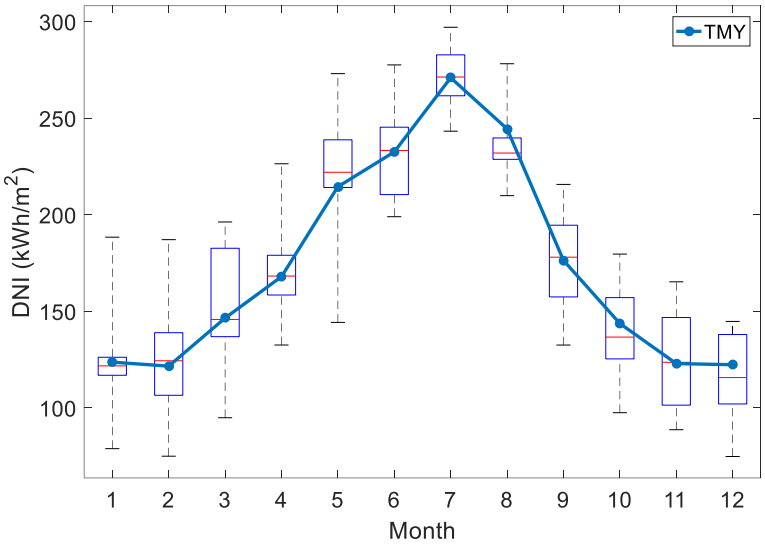

We observe that the monthly cumulative values of the TMY (the blue dots) are close to the median (the horizontal red lines). The monthly distribution has an inverted V-shape, where the maximum is found in July, and the minimum in winter. It is noteworthy that Seville has a Mediterranean climate, with higher variability from January to May (as shown by the extension of their ranges), and that TMY is specific to location.

The statistical characterization of the solar resource and their uncertainties play significant roles in financing solar power projects. Financial entities and their shareholders need to know the uncertainty levels of yield estimates to evaluate risks associated with their investments. The uncertainty in solar resource assessments impacts the uncertainty of the yield estimates. This uncertainty has two main sources, the uncertainty of the data, and the uncertainty associated with the variability of the solar resource, which is not captured by single-year TMYs.

The uncertainty of the data depends on the quality of the sensors and their maintenance for ground measurements derived series. In the case of satellite-derived data, it depends on the model and the site adaptation procedures used, being location-dependent and having a higher uncertainty than measured data.

The uncertainty associated with variability can be defined by the inter-annual variability of solar radiation. A common practice to cope with uncertainty

associated with the variability is to evaluate the project's energy yield using as input single-year time series corresponding to unfavorable scenarios in years with a high probability of exceedance (PoE). The yield estimates obtained for these years are used by investors and lenders to assess a project's ability to manage risks and to meet their return requirements [65].

High PoE series that are used to model these scenarios are generally calculated alongside TMYs (which usually correspond to the PoE50) in feasibility assessments of solar projects. The procedures proposed by the UNE 206013:2017 standard [97] to build PoE series for CSP projects consist of the following steps:

- Calculating which distribution function is best suited to the observed annual values and obtaining the annual values that correspond to the required PoEs from the distribution. Annual GHI values are assumed to follow normal distributions, while annual DNIs tend to follow Weibull distributions [18].
- Estimating monthly values of the required PoEs. A common practice is to calculate the difference between the annual value of the corresponding PoE and the TMY, and then to distribute this difference to each month proportionally to the standard deviations of the monthly series [53].
- Constructing the PoE series by concatenating daily observed sets to match their corresponding estimated PoE monthly values.

The TMY and the PoE monthly distributions for Seville usually present an inverted V-shape, with relatively smooth and progressive changes from one month to the next, taking monthly values between the minimum and the maximum ones available in the long-term time series (typically fifteen or twenty years), as they are selected to represent the most probable annual data set corresponding to that specific PoE at annual scale. For that reason, they do not include extreme monthly values that might occur and that may not be present in long-term databases. In Figure 5 we present the monthly values and the TMY observed in Seville, Spain, over fifteen years in a box plot, with the TMY, the PoE 90 and the PoE 99.

Fig 5. Box plot of observed monthly DNI values with calculated TMY, PoE90 and PoE99 in Seville, Spain.

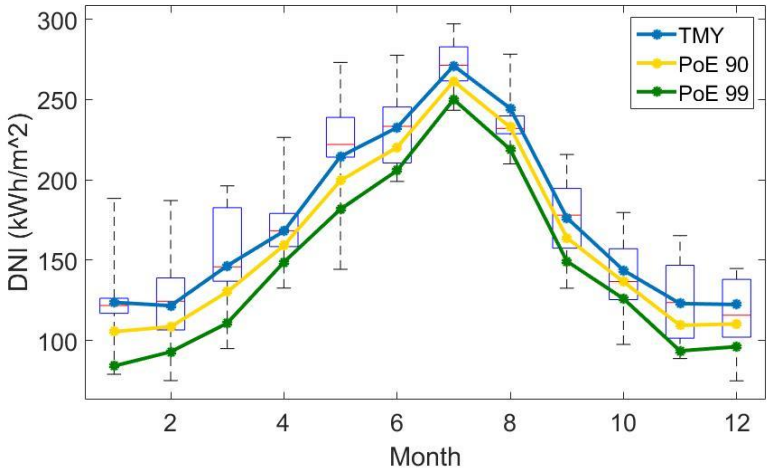

While the TMY and PoE99 monthly DNI values show a characteristic inverted V-shape, this is not common for observed values. In fact, most annual sets include monthly values that are lower or higher than those of synthetic series. The shape of the monthly distribution of annual sets is usually more complex than that of the PoEXX series that is illustrated in Figure 6, which presents the monthly values observed in 2015 with the TMY and the PoE99. We also present the PoE of each monthly value within its monthly observed data set. The annual DNI in 2015 was slightly greater than the TMY corresponding value (2160 vs. 2088 kWh/m2), but there are four monthly values above the PoE25, and another four below the PoE75. In addition, the August and October values are lower than those of the PoE99 series.

Fig 6. Monthly distribution of DNI for TMY and PoE99, with monthly values for 2015, which has an annual cumulative value that is similar to that of the TMY. The blue text boxes beside the markers of the year indicate the value of the probability of exceeding the observed monthly value.

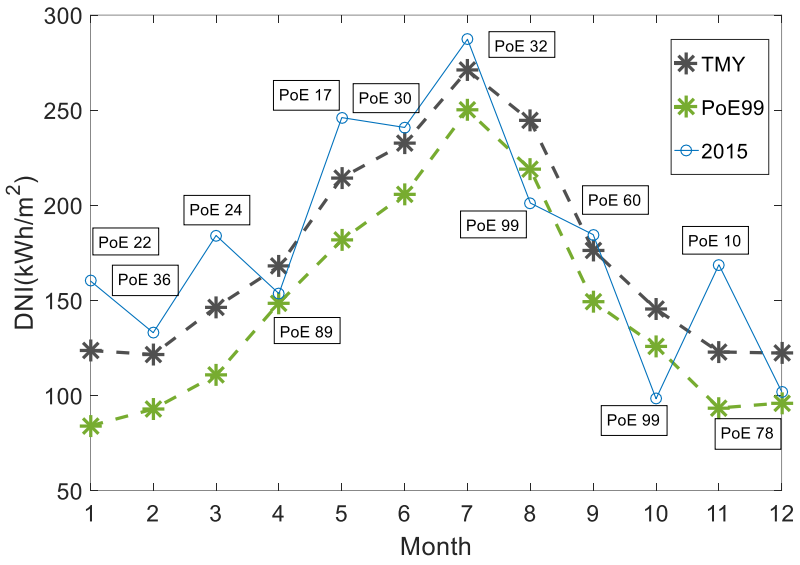

3.3 Solar resource characterization by means of multiple annual synthetic sets

The characterization of the solar resource by means of single-year series such as TMY or PoE50 involves a loss of the information contained in the original time series. Nowadays, advances in computer technology and modelling of solar energy systems allow us to make use of the whole original time series to simulate the performance of a solar energy plant and analyze the results with minimal effort. But even the original time series, unless they comprise a very large number of years, may not be able to represent potential solar resource scenarios and changes (for example, those associated with climate change) that might occur during a project's lifetime.

The research community is currently addressing this issue, and several approaches have already been tested and presented in the literature, such as the multiyear approach proposed by Nielsen, et al. [19]. The synthetic generation of time series of solar radiation and other (possibly coupled) meteorological parameters, presented in Section 2 of this chapter, constitutes a valuable tool for this purpose.

In a recent paper, Larrañeta, et al. [38] presented a promising globally applicable method for the synthetic generation of multiple annual solar radiation time series in

high resolution (one-minute). The application of the method requires ten to fifteen annual time series of hourly DNI and GHI values that can be retrieved from satellite-based or reanalysis irradiance databases for most of the locations on earth [98], and generates 100 annual sets (Plausible Meteorological Years, or PMYs) of one-minute coupled GHI and DNI time series. It consists of the concatenation of three steps of generating synthetic values. In the first step, a bootstrapping technique is used to generate synthetic monthly values from cumulative distribution functions (CDFs) of the observed monthly values. Then, the synthetically generated monthly values are combined to produce 100 synthetic years, each consisting of twelve synthetic monthly values (one per month of the year). Although the bootstrapping technique ensures that synthetic monthly values of solar radiation lower or greater than the values present in the input time series are never generated, the annual solar radiation values of the synthetic years can be greater or lesser than corresponding annual values from the input series. The last two steps consist of the generation of synthetic daily and one-minute values for each month of the synthetic sets, using the synthetic generation techniques presented earlier.

This method extends the range of potential scenarios with respect to the observed ones, ensuring that the statistical characteristics observed in the input series are maintained. The resulting synthetic data sets can be used for feasibility assessments of solar projects to help engineers assess solar radiation variability and its impact on solar energy systems.

In the case that we present here, we use the same fifteen years of one-minute DNI data measured in Seville described in Section 4.1 to generate 100 synthetic years of one-minute DNI values. In Figure 7 we present the box plots of the observed annual DNI values and the synthetically generated annual DNI values.

Fig 7. Box plot of fifteen annual values and 100 synthetically generated annual values.

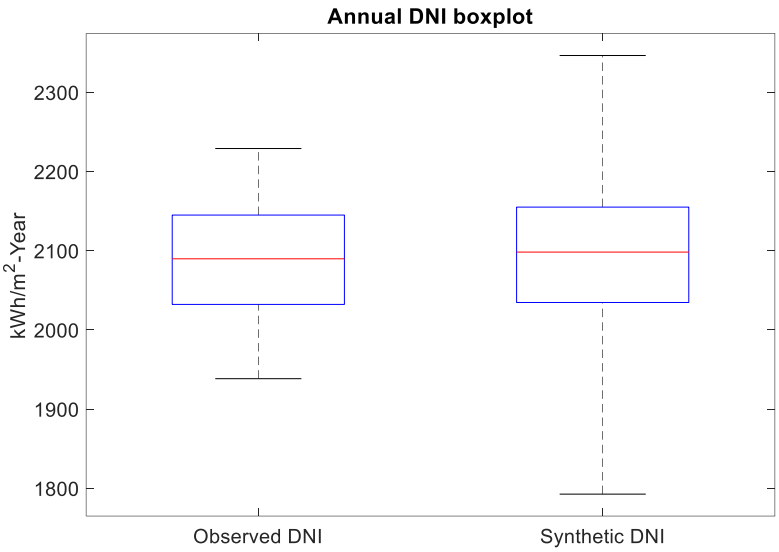

In Figure 7 we observe that the range of annual values is wider for the synthetic data set. The minimum and maximum annual DNI values of the observed data set are 1938 kWh/m2 and 2229 kWh/m2, respectively; the synthetic data sets have a minimum of 1792 kWh/m2 and a maximum of 2345 kWh/m2. There are nine synthetic years with values that are out of the range of the observed values, which represent scenarios statistically compatible with the observed data, but not present in the observed data set. This is the critical purpose for PMY. The data suggests that all PMY are entirely plausible, yet the observation data did not have the opportunity to measure such a year, hence, relying on these 15 years could miss those 1 in 100 events, or in this case, 9 in 100.

3.4 Performance evaluation of the Andasol 3 solar plant using single synthetic and multiple synthetic sets as inputs on an annual and monthly basis

The performance evaluation of a solar plant consists of the assessing different scenarios determined by several time series of solar radiation, which is the main input for the solar energy systems. In performance evaluations of CSP plants, a common approach is to estimate the gross production from the solar plant using different solar radiation data sets as input, whether observed or synthetic. The gross

production is the power delivered by the generating unit before subtracting self-consumption power. In this section we evaluate the performance of Andasol 3 solar plant on an annual and monthly basis in the scenarios defined by the simple synthetic data sets (TMY, PoE90 and PoE99) and the multiple synthetic PMY approach.

The evaluation of the gross generation values obtained from simulating the CSP plant with the observed and synthetic simple and multiple sets as inputs is presented in this Section.

The multiple synthetic sets methodology, or multiyear approach (see Section 3.3) lead to the generation of 100 synthetic annual sets corresponding to different levels of annual solar radiation, from very low to very high, leading to what we call in the next figures, plausible meteorological years or PMYs.

Figure 8 shows the annual gross production in a scatter plot versus the annual DNI. We present the annual gross production obtained from running simulations using the observed data sets (red triangles), the PMYs (empty blue circles), and the single synthetic data set, TMY (blue dot), PoE90 (yellow dot) and PoE99 (green dot). We present the annual DNI and gross production numerical values of the TMY, PoE90 and PoE99 in the plot. We also present the least-squares fit on a dotted black line.

Fig 8. Scatter plot of the gross production versus the annual DNI for simulations of Andasol 3 performance evaluation using observed and synthetic sets as inputs. Observed sets are presented with red triangles, PMY sets with empty blue dots, the TMY with a blue dot, the PoE90 with a yellow dot and the PoE99 with a green dot. We also present the least-squares fit with a dotted black line.

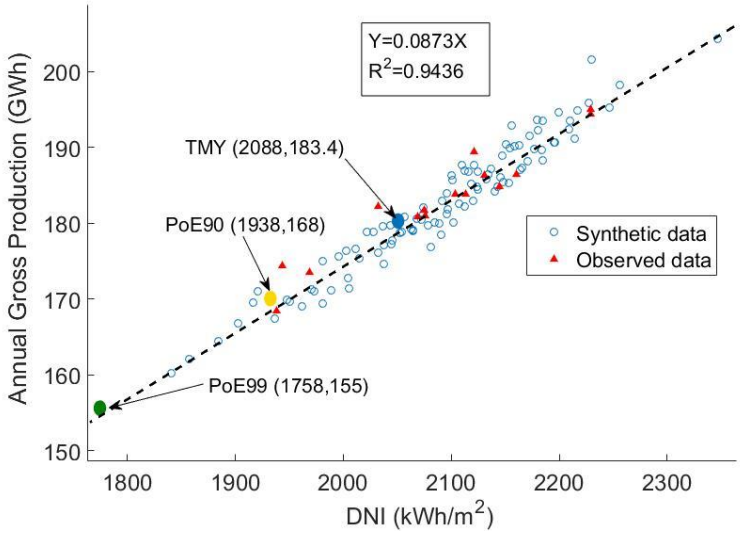

Note that the single synthetic annual sets represent the expected performance of the solar plant in three characteristic scenarios: an average production (TMY with a blue dot), a bad case (PoE90 with a yellow dot) and the worst case (PoE99 with a green dot). The observed sets (red triangles) are mostly distributed along average annual values (2050-2150 kWh/m^2-year), and only few of them represent extreme cases. The worst observed value is similar to the estimated PoE90. This might be explained in that the observed sample represents a period of fourteen years (see table 2), in which extreme years might not have appeared.

There is an almost linear relation between the annual solar radiation and the annual gross production of the Andasol 3 solar plant, but if we focus on the PMYs (empty blue dots), there is an uncertainty related to the impact of the monthly distribution of the solar radiation. For an annual DNI value near the average (DNI $\approx$ 2100 $\pm$ 20 kWh/m^2-year), we obtain a range of gross production values between 178-185 GWH-year. From these results, we could estimate an uncertainty value in the expected gross production for a single solar radiation annual set related to the monthly and daily variability of the solar radiation.

In Figure 9 we present the estimated annual gross production of Andasol 3 versus the annual DNI of the PMY series in a box plot figure. Each box contains ten annual sets with similar annual cumulative DNI values. For instance, the box representing the PoE10 corresponds to the annual gross production obtained when performing simulations using ten DNI annual sets from PoE06 annual set to PoE15 annual set.

In Figure 9, we also present the TMY (blue dot), the single synthetic PoE90 (yellow dot), the single synthetic PoE99 (green dot), and the numerical value of the PoE20, PoE50 and PoE80 of DNI with a dashed blue line. This way we can visualize the range of gross production values that we can obtain by running simulations with solar data sets with similar annual cumulative values, but with different monthly and daily distributions.

Fig 9. Box plots of annual gross power as a function of annual DNI synthetic sets. Each box contains ten annual sets with similar annual cumulative DNI values. The PoE20, PoE50, and PoE80 values are numerically presented and diagrammed with a dashed blue line. The gross production obtained using the single synthetic solar radiation sets as input for the simulations is also presented in colored dots. A blue dot represents the TMY, a yellow dot represents the PoE90, and a green dot represents the PoE99.

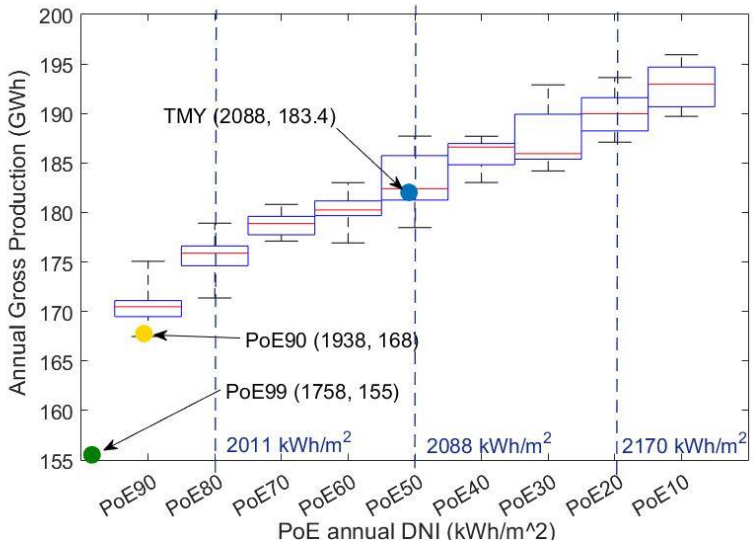

The single synthetic sets, TMY, PoE90 and PoE99 presented in blue, yellow and green dots, respectively, accurately represent the expected performance of the plant under average, bad and worst-case scenarios. The TMY overlaps the red line of the PoE50 box, and the PoE90 single synthetic set overlaps at the minimum values of the PoE90 box. The PoE99 can be evaluated in Figure 9, but from Figure 8 we observe that it follows the linear relation that is obtained from a least-square fit.

At this point we would like to direct the reader's attention to the relevance of the reproduction of the variability of the solar radiation in the synthetic generation of

solar data sets, as it has a remarkable impact on the estimation of the production of solar plants. In Figure 10 we present the gross production monthly distribution of the single synthetic sets TMY (blue line), PoE90 (yellow line), and PoE99 (green line) with the gross production of the PMYs presented in a box plot.

Fig 10. Box plot of the gross production of A3 obtained using the PMY synthetic 100 annual data sets (box plot) with the gross production obtained using the single synthetic sets TMY (blue line), PoE90 (yellow line) and PoE99 (green line) data sets as input.

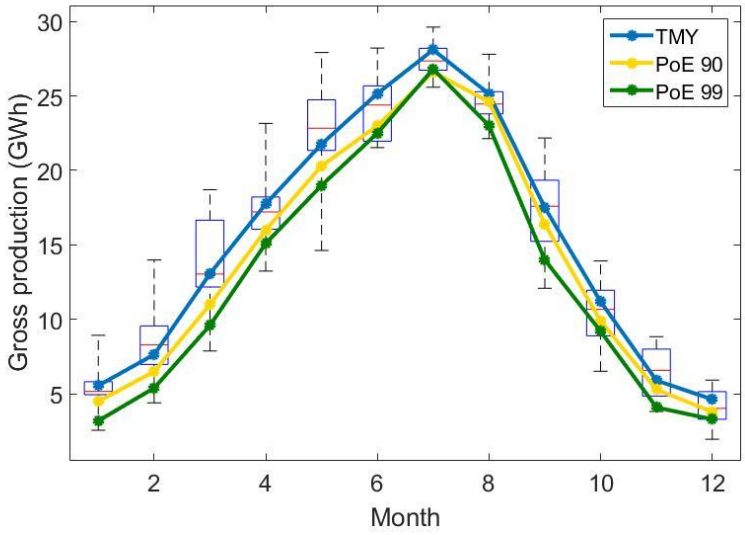

In Figure 10 we can observe the similarity between the production of the single annual set approach and the median value of the multiyear approach (red line of each box) for most of the cases. Note that for the northern summer months (June, July and August), the TMY is closer to the upper bound of the box that represents the PoE25 of the synthetic PMYs. In the case of extreme years, PoE90 and PoE99, we can see a significant overestimation of the power production in comparison to the multiyear approach, especially during the northern spring and autumn months of March, April, May, September and October. The single year approach for the extreme cases provides average bad case scenarios, while with the multiyear approach, the observed worst monthly cases are included. This issue becomes especially relevant in those months with a high variability such, such as those mentioned before.

It is noteworthy that the PoE99 represents the worst-case scenario in terms of annual cumulative DNI, but it is not necessarily the worst-case in terms of monthly production values. In fact, in most months, the single synthetic PoE99 gross production value is greater than the minimum monthly gross production value that is obtained with the PMY approach.

3.5 Performance evaluation of the Andasol 3 solar plant using single synthetic and multiple synthetic sets as inputs on daily and hourly scales

The performance evaluation of solar plants is generally addressed across various temporal resolutions. In Section 3.4, we evaluated the performance of Andasol 3 over annual and monthly resolutions, but it is also interesting to evaluate the performance at daily and higher available resolutions (perhaps at scales of one minute or one hour).

Most of the statistical quantifiers used to evaluate the success of synthetic irradiance production are calculated from data at these time resolutions. These quantifiers are useful for finding similarities between observed and synthetic sets, but in some cases, synthetic sets are not expected to match observed sets, but instead to represent different scenarios, such as averages or extremes. In this case, a visual assessment to evaluate the success of synthetic time series is recommended. In this Section, we calculate cumulative distribution functions (CDFs) of synthetic sets over observed sets at daily and hourly resolutions. The cumulative distribution function is the probability that a random variable is less than or equal to a certain value. For more information about validating synthetic data sets, refer to Chapter 4.

In the case of feasibility assessments of solar projects using single (TMY, PoE90, PoE99) or multiple (PMYs) annual sets, a visual inspection of the CDFs of observed and synthetic sets is recommended to inspect similarities between the data sets in terms of solar radiation and/or gross production. In Figure 11 we represent the CDF of the synthetic single and multiple solar radiation data sets with the CDFs of the observed solar radiation data sets at a daily resolution at Andasol 3's location. The

observed data sets are presented with red lines, the PMYs are presented with light blue lines, the TMY is presented with a blue line, the single synthetic PoE90 is presented with a yellow line, and, finally, the PoE99 is presented with a green line. This color code applies to Figures 11 through14 below.

Fig 11. CDFs of observed (red lines) and synthetic DNI data sets at daily resolution for Andasol 3. Light blue lines represent PMYs, blue lines represent TMY, yellow lines represent the single synthetic PoE90, and a green line represents the single synthetic PoE99.

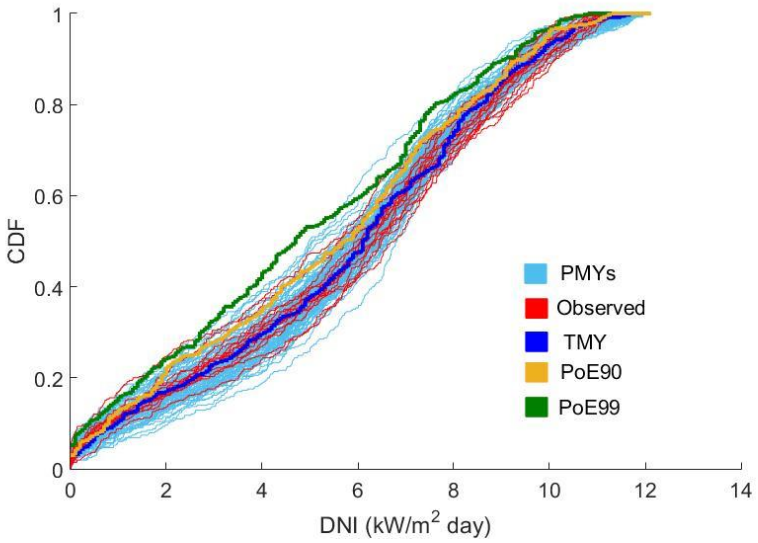

Visualizing the CDFs of solar data set, we can extract quite a lot of information. The Y-axis ranges from 0 to 1, while the X-axis ranges from the minimum to the maximum daily value. The 0 of the Y-axis correlates to the minimum value of the X-axis. The 1 of the Y-axis correlates to the maximum daily value. The shape of the CDF provides information about the distribution of the data set. For instance, if we trace a vertical straight line from the X-axis' value of 5.0 kWh/m^2-day, we find CDF values that range from 0.25 to 0.5, meaning that for the clearest annual set, the probability that a daily value is lower than or equal to 5.0 kWh/m^2-day is 25%, and that for the worst case annual set, the probability that a daily value is lower than or equal to 5.0 kWh/m^2-day is 50%. These values are identified in the PMYs and the simple synthetic PoE99, respectively. In light of this analysis, the CDF profiles that tilt towards the bottom of the Y-axis represent data sets with relatively higher levels

of solar radiation. On the other hand, the CDF profiles that tilt towards the upper portion of the Y-axis represent data sets with lower levels of solar radiation.

As shown in Figure 11, the TMY presents an average CDF with respect to the CDFs of the observed data sets, since it is located in the middle of the space occupied by the CDFs of the observed sets. The PMY CDFs present a greater range of scenarios than the observed sets, including bad and worst-case scenario CDFs similar to the single synthetic (PoE90 and PoE99) annual sets.

Figure 12 shows the CDF of the synthetic single and multiple solar radiation data sets with the CDFs of the observed solar radiation data sets at the daily resolution for the location of Andasol 3.

Fig 12. CDFs of the observed (red lines) and synthetic DNI data sets at an hourly resolution for Andasol 3. The PMYs are presented with light blue lines, the TMY is presented with a blue line, the single synthetic PoE90 is presented with a yellow line and the single synthetic PoE99 is presented with a green line.

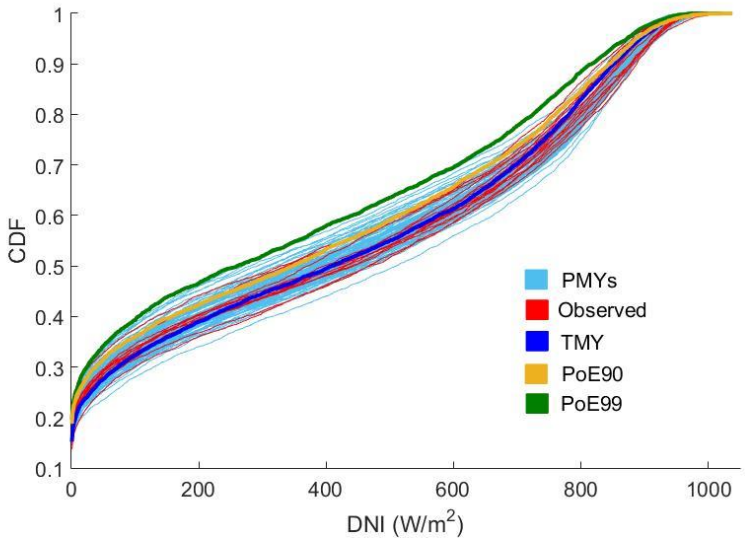

At one-hourly resolution, we observe that the PMYs expand the observed scenarios by covering a wider portion of the plot, but do not present any annual set that reaches the low values observed in the CDF of the single synthetic set PoE99 which clearly defines the worst-case scenario as represented by the uppermost CDF profile. This trend can also be observed at the daily resolution in Figure 11. We also

observe that, at the hourly time resolution, the CDF of the single synthetic PoE90 is very similar to the CDF of the TMY since both of them are mostly overlapped.

The CDFs of the solar radiation data sets are generally evaluated because it is assumed that the distribution of the data set has a great impact in the production of the solar plants especially in those that use the direct component of the solar radiation such as the CSP plants. We obtain gross production estimations of Andasol 3 solar plant at the hourly resolution, thus we can plot the CDFs in terms of gross production and address the performance assessment in these terms and compare the CDFs of gross production to the CDFs of solar radiation. In Figure 13 we present the CDFs of the daily gross production obtained when running simulations using the observed and synthetic data sets.

Fig 13. CDFs of the observed (red lines) and synthetic gross production data sets at a daily resolution for Andasol 3. The PMYs are presented with light blue lines, the TMY is presented with a blue line, the single synthetic PoE90 is presented with a yellow line and the single synthetic PoE99 is presented with a green line.

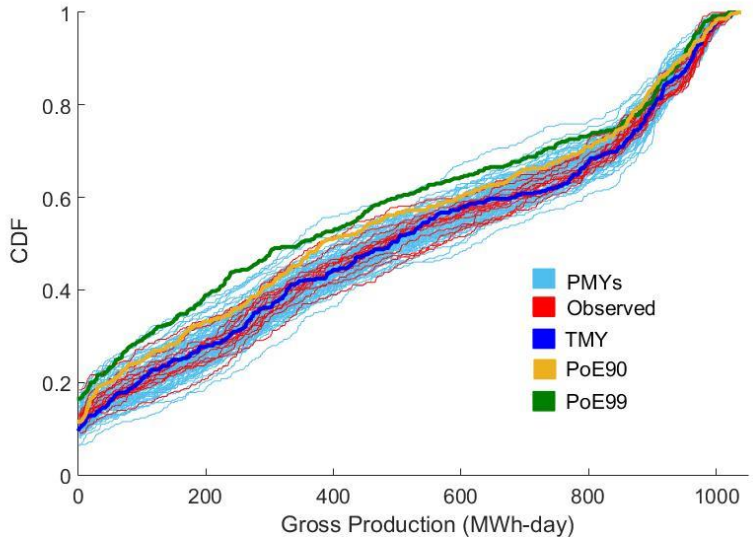

In Figure 13 we observe tendencies that are similar to those of Figure 11, but with slight differences. We can assume that what we find in the CDFs of daily solar radiation data sets can be extrapolated to CDFs of daily gross production. We find that the TMY still presents an average CDF in relation to the CDFs of the observed data sets. The PMY CDFs still present a greater range of scenarios than the observed

sets including bad and worst-case scenario CDFs similar to the single synthetic (PoE90 and PoE99) annual sets. The single synthetic PoE99 still properly represents the worst-case scenario but, this time, in terms of gross production, the PoE99 and the PoE90 single synthetic data sets are almost overlapped. There is no great differences between the CDFs of both data sets.

In Figure 14 we present the CDFs of the hourly gross production obtained from simulations with observed and synthetic data sets.

Fig 14. CDFs of the observed (red lines) and synthetic gross production data sets at an hourly resolution for Andasol 3. The PMYs are presented with light blue lines, the TMY is presented with a blue line, the single synthetic PoE90 is presented with a yellow line and the single synthetic PoE99 is presented with a green line.

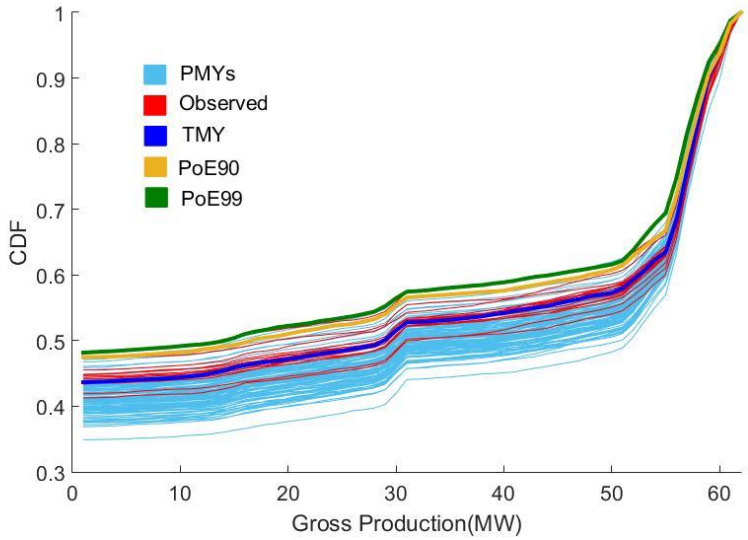

In Figure 14 we observe that the hourly gross production CDFs of the single synthetic PoE90 and PoE99 sets present slight differences. The CDFs of PMYs (light blue lines) cover the bottom part of Figure 14, which suggests a slight tendency to overestimate the hourly production. While there is a general similarity between the daily solar radiation and gross production CDFs, (Figure 11 and Figure 13, respectively), the CDF profiles of solar radiation and gross production at the hourly resolution (Figure 12 and Figure 14) do not coincide. This might be explained by a dampening effect from the thermal storage system in the gross production of the solar plant. If we focus on the CDF gross production profiles at

an hourly resolution, and if we trace a vertical line from the gross production value of the X-axis at 50MW, we find that most of the CDFs' values range from 0.45 to 0.55, which means that plant works below the nominal power in around 50% of the occurrences. Thus, the plant functions near its nominal power in the other 50% of occurrences. Functioning near nominal power is the general aim of all the thermal conversion systems. Due to the intermittency of solar radiation, CSP systems find difficulties in working continuously near nominal power. Thermal storage system capacity and the over dimensioning of the solar field (see table 1) dampens the impact of the cloud transients and allows the plant to work near the nominal power for more time.

4 Summary and Conclusions

In this chapter, we covered topics around synthetic irradiance generation for industrial and commercial application purposes, particularly with DNI generation for CSP plants. We carried out a case study for a CSP solar plant that is located in the city of Seville in the south of Spain. We aimed to explain the possibilities and uses of synthetic irradiance in industrial application with a focus upon the requirements in the characterization of the solar radiation potential from the industry stakeholder's point of view, explaining common approaches for the synthetic data generation for industrial applications.

Temporal-only time series of solar irradiance measurements are widely used to assess the expected performances of solar energy collection systems over the course of such systems' lifetimes and on the grid impact analysis and urban DG planning. It is also worth noting a growing interest in other areas such as building energy consumption reduction. Solar industry stakeholders, that is, developers, financers, researchers, operators, etc., require long solar time series that are not usually available from local observations at sites of interest. Synthetic solar irradiance is, in many cases, actually used to meet this need showing particular usefulness in the present and significant potential in the near and long future.

We presented a case study that assessed the solar yield of Andasol 3, a parabolic trough solar plant that is located in the southern Spanish city of Seville. We have performed a feasibility assessment through a common approach by calculating

single synthetic annual sets that respectively represent average, bad and worst-case scenarios (TMY, PoE90 and PoE99) as well as a novel approach based upon the generation of plausible meteorological years (PMYs). The assessment was performed in terms of both solar radiation and produced power. The results showed that a single-year approach provided a suitable description of typical and worst-case scenarios, however, these simpler approaches did not reproduce the solar radiation's inherent intra-annual variability, which is particularly relevant in some applications such as concentrated solar energy systems or hybrid systems with a base load minimum requirement. The PMY approach reproduced the solar resource variability at both short-term and long-term scales and provided a range of possibilities that were suitable and facilitating of a more comprehensive performance assessment of solar energy systems.

The PMY approach exhibits a promising usefulness in the future of solar energy harnessing systems. The next chapter expands upon future outlooks in the field of synthetic solar irradiance.

5 Acknowledgments

This work has been carried out in the frame of the project "Development of a prototype for the creation of a technology-based company based on the concept of "Multiyear synthetic generation" funded by the *Junta de Andalucía* (Spain) in the frame of the Andalusian investigation development and innovation plan (PAIDI 2020).

References

1. Kim, K.-K.; Lee, C.-G. Evaluation and optimization of feed-in tariffs. *Energy Policy* **2012**, *49*, 192–203, doi:10.1016/j.enpol.2012.05.070.
2. Couture, T.; Gagnon, Y. An analysis of feed-in tariff remuneration models: Implications for renewable energy investment. *Energy Policy* **2010**, *38*, 955–965, doi:10.1016/j.enpol.2009.10.047.
3. del Río González, P. Ten years of renewable electricity policies in Spain: An analysis of successive feed-in tariff reforms. *Energy Policy* **2008**, *36*, 2917–2929, doi:10.1016/j.enpol.2008.03.025.
4. Avril, S.; Mansilla, C.; Busson, M.; Lemaire, T. Photovoltaic energy policy: Financial estimation and performance comparison of the public support in five representative countries. *Energy Policy* **2012**, *51*, 244–258, doi:10.1016/j.enpol.2012.07.050.

5. Engeland, K.; Borga, M.; Creutin, J.-D.; François, B.; Ramos, M.-H.; Vidal, J.-P. Space-time variability of climate variables and intermittent renewable electricity production – A review. *Renew. Sustain. Energy Rev.* **2017**, *79*, 600–617, doi:10.1016/j.rser.2017.05.046.
6. Schill, W.-P. Residual load, renewable surplus generation and storage requirements in Germany. *Energy Policy* **2014**, *73*, 65–79, doi:10.1016/j.enpol.2014.05.032.
7. Sengupta, M.; Habte, A.; Gueymard, C.; Wilbert, S.; Renne, D. *Best practices handbook for the collection and use of solar resource data for solar energy applications*; National Renewable Energy Lab.(NREL), Golden, CO (United States), 2017;
8. Climate Normals | National Centers for Environmental Information (NCEI) formerly known as National Climatic Data Center (NCDC) Available online: https://www.ncdc.noaa.gov/data-access/land-based-station-data/land-based-datasets/climate-normals (accessed on Jan 14, 2020).
9. Mulder, F.M. Implications of diurnal and seasonal variations in renewable energy generation for large scale energy storage. *J. Renew. Sustain. Energy* **2014**, *6*, 33105, doi:10.1063/1.4874845.
10. Lüpfert, E.; Geyer, M.; Schiel, W.; Esteban, A.; Osuna, R.; Zarza, E.; Nava, P. EuroTrough Design Issues and Prototype Testing at PSA.; American Society of Mechanical Engineers Digital Collection, 2020; pp. 387–391.
11. Rahman, M.M.; Hasanuzzaman, M.; Rahim, N.A. Effects of various parameters on PV-module power and efficiency. *Energy Convers. Manag.* **2015**, *103*, 348–358, doi:10.1016/j.enconman.2015.06.067.
12. Bright, J.M. Development of a synthetic solar irradiance generator that produces time series with high temporal and spatial resolutions using readily available mean hourly observations. phd+master, University of Leeds, 2017.
13. Reikard, G. Predicting solar radiation at high resolutions: A comparison of time series forecasts. *Sol. Energy* **2009**, *83*, 342–349, doi:10.1016/j.solener.2008.08.007.
14. Chow, C.W.; Urquhart, B.; Lave, M.; Dominguez, A.; Kleissl, J.; Shields, J.; Washom, B. Intra-hour forecasting with a total sky imager at the UC San Diego solar energy testbed. *Sol. Energy* **2011**, *85*, 2881–2893, doi:10.1016/j.solener.2011.08.025.
15. Yang, D.; Jirutitijaroen, P.; Walsh, W.M. Hourly solar irradiance time series forecasting using cloud cover index. *Sol. Energy* **2012**, *86*, 3531–3543, doi:10.1016/j.solener.2012.07.029.
16. Lukhyswara, P.; Putranto, L.M.; Ariananda, D.D. Solar Irradiation Forecasting Uses Time Series Analysis. In Proceedings of the 2019 11th International Conference on Information Technology and Electrical Engineering (ICITEE); 2019; pp. 1–6.
17. Vignola, F.; McMahan, A.; Grover, C. Evaluation of Resource Risk in Solar-Project Financing. In *Solar Energy Forecasting and Resource Assessment*; Academic Press, 2013.
18. Fernández Peruchena, C.M.; Ramírez, L.; Silva-Pérez, M.A.; Lara, V.; Bermejo, D.; Gastón, M.; Moreno-Tejera, S.; Pulgar, J.; Liria, J.; Macías, S.; et al. A statistical characterization of the long-term solar resource: Towards risk assessment for solar power projects. *Sol. Energy* **2016**, *123*, 29–39, doi:10.1016/j.solener.2015.10.051.
19. Coimbra, C.F.M.; Kleissl, J.; Marquez, R. Chapter 8 - Overview of Solar-Forecasting Methods and a Metric for Accuracy Evaluation. In *Solar Energy Forecasting and Resource Assessment*; Academic Press: Boston, 2013; pp. 171–194 ISBN 978-0-12-397177-7.
20. Lave, M.; Kleissl, J. Solar variability of four sites across the state of Colorado. *Renew. Energy* **2010**, *35*, 2867–2873, doi:10.1016/j.renene.2010.05.013.
21. Schepanski, K.; Klüser, L.; Heinold, B.; Tegen, I. Spatial and temporal correlation length as a measure for the stationarity of atmospheric dust aerosol distribution. *Atmos. Environ.* **2015**, *122*, 10–21, doi:10.1016/j.atmosenv.2015.09.034.

22. Meyer, R.; Beyer, H.G.; Fanslau, J.; Geuder, N.; Hammer, A.; Hirsch, T.; Hoyer-Klick, C.; Schmidt, N.; Schwandt, M. Towards standardization of CSP yield assessments. In Proceedings of the Conference paper: SolarPACES; 2009.
23. Hirsch, T.; Schenk, H.; Schmidt, N.; Meyer, R. Dynamics of oil-based parabolic trough plants—Impact of transient behaviour on energy yields. In Proceedings of the Proc. SolarPACES Conf., Perpignan, France; 2010.
24. Kemper, A.; Lorenz, E.; Hammer, A.; Heinemann, D. Evaluation of a new model to calculate direct normal irradiance based on satellite images of Meteosat Second Generation. In Proceedings of the Proceedings of the EUROSUN 2008 1st International Conference on Solar Heating, Cooling and Buildings; 2008.
25. Polo, J.; Zarzalejo, L.F.; Marchante, R.; Navarro, A.A. A simple approach to the synthetic generation of solar irradiance time series with high temporal resolution. *Sol. Energy* **2011**, *85*, 1164–1170, doi:10.1016/j.solener.2011.03.011.
26. Beyer, H.-G.; Fauter, M.; Schumann, K.; Schenk, H.; Meyer, R. Synthesis of DNI time series with sub-hourly time resolution. In Proceedings of the Proceedings SolarPACES 2010; Perpignan, France, 2010.
27. Fernández-Peruchena, C.M.; Blanco, M.; Gastón, M.; Bernardos, A. Increasing the temporal resolution of direct normal solar irradiance series in different climatic zones. *Sol. Energy* **2015**, *115*, 255–263, doi:10.1016/j.solener.2015.02.017.
28. Larrañeta, M.; Moreno-Tejera, S.; Silva-Pérez, M.A.; Lillo-Bravo, I. An improved model for the synthetic generation of high temporal resolution direct normal irradiation time series. *Sol. Energy* **2015**, *122*, 517–528.
29. Fernández Peruchena, C.M.; Gastón, M.; Schroedter-Homscheidt, M.; Kosmale, M.; Martínez Marco, I.; García-Moya, J.A.; Casado-Rubio, J.L. Dynamic Paths: Towards high frequency direct normal irradiance forecasts. *Energy* **2017**, *132*, 315–323, doi:10.1016/j.energy.2017.05.101.
30. Hummon, M.; Ibanez, E.; Brinkman, Gregory; Lew, Debra Sub-Hour Solar Data for Power System Modeling From Static Spatial Variability Analysis.; National Renewable Energy Laboratory: Lisbon, Portugal, 2012.
31. Helman, U.; Loutan, C.; Rosenblum, G.; Guo, T.; Toolson, E.; Hobbs, B. Integration of renewable resources: Updated analysis of operational requirements and assessment of generation fleet capability under a 20% RPS requirement. In Proceedings of the IEEE PES General Meeting; 2010; pp. 1–2.
32. Nielsen, K.P.; Vignola, F.; Ramírez, L.; Blanc, P.; Meyer, R.; Blanco, M. Excerpts from the report: "BeyondTMY - Meteorological data sets for CSP/STE performance simulations." *AIP Conf. Proc.* **2017**, *1850*, 140017, doi:10.1063/1.4984525.
33. Fernández-Peruchena, C.M.; Gastón, M.; Sánchez, M.; García-Barberena, J.; Blanco, M.; Bernardos, A. MUS: A multiscale stochastic model for generating plausible meteorological years designed for multiyear solar energy yield simulations. *Sol. Energy* **2015**, *120*, 244–256, doi:10.1016/j.solener.2015.07.037.
34. Meybodi, M.A.; Santigosa, L.R.; Beath, A.C. A study on the impact of time resolution in solar data on the performance modelling of CSP plants. *Renew. Energy* **2017**, *109*, 551–563.
35. Ho, C.K.; Khalsa, S.S.; Kolb, G.J. Methods for probabilistic modeling of concentrating solar power plants. *Sol. Energy* **2011**, *85*, 669–675, doi:10.1016/j.solener.2010.05.004.
36. Ho, C.K.; Kolb, G.J. Incorporating Uncertainty into Probabilistic Performance Models of Concentrating Solar Power Plants. *J. Sol. Energy Eng.* **2010**, *132*, 031012–031012, doi:10.1115/1.4001468.
37. Benseman, R.F.; Cook, F.W. Solar Radiation in New Zealand-Standard Year and Radiation on Inclined Slopes. *N. Z. J. Sci.* **1969**, *12*, 696-.
38. Petrie, W.R.; McClintock, M. Determining typical weather for use in solar energy simulations. *Sol. Energy* **1978**, *21*, 55–59, doi:10.1016/0038-092X(78)90116-0.
39. Feuermann, D.; Gordon, J.M.; Zarmi, Y. A typical meteorological day (TMD) approach for predicting the long-term performance of solar energy systems. *Sol. Energy* **1985**, *35*, 63–69, doi:10.1016/0038-092X(85)90037-4.

40. Lund, H. *Short Reference Years - Test Reference Years*; Commission of the European Communities, Luxembourg, 1984;
41. Lund, H. *The" Reference Year", a set of climatic data for environmental Engineering*; Thermal Insulation Laboratory, Technical University of Denmark, 1974;
42. Andersen, B.; Eidorff, S.; Hallgreen, L.; Lund, H.; Pedersen, E.; Rosenoern, S.; Valbjoern, O. [Meteorological data for HVAC and energy: Danish test reference year TRY [15-year period, outdoor climate heating, ventilation, heat balances, solar heating]]. *SBI Rapp. Den.* **1982**.
43. Festa, R.; Ratto, C.F. Proposal of a numerical procedure to select Reference Years. *Sol. Energy* **1993**, *50*, 9–17, doi:10.1016/0038-092X(93)90003-7.
44. *Test reference year (TRY), in: Tape Reference Manual*; Asheville, NC, USA; National Climatic Data Center, 1976;
45. Andersen, B.; Eidorff, S.; Lund, H.; Pedersen, E.; Rosenoern, S.; Valbjoern, O. *Referenceåret - Vejrdata for VVS beregninger (The Reference Year - Weather data for HVAC-calculations)*; Danish Building Research Institute, 1974;
46. Hall, L.; Prairie, R.; Anderson, H.; Boes, E. *Generation of Typical Meteorological Years for 26 SOLMET stations*; Sandia National Lab.: Albuquerque, NM., 1978;
47. Lund, H. *The design reference year user manual, a report of Task 9: Solar radiation and pyranometer studies. Solar Materials Research and Development, International Energy Agency Solar Heating and Cooling Programme*; Report No. IEA-SHCP-9E-1, Report, 1995;
48. Finkelstein, J.M.; Schafer, R.E. Improved Goodness-Of-Fit Tests. *Biometrika* **1971**, *58*, 641–645, doi:10.2307/2334400.
49. Marion, W.; Urban, K. *Users manual for TMY2s: Derived from the 1961--1990 National Solar Radiation Data Base*; National Renewable Energy Lab., Golden, CO (United States), 1995;
50. Wilcox, S.; Marion, W. Users manual for TMY3 data sets. **2008**.
51. *The Performance of Concentrated Solar Power (CSP) Systems*; Elsevier, 2017; ISBN 978-0-08-100447-0.
52. Habte, A.; Lopez, A.; Sengupta, M.; Wilcox, S. *Temporal and Spatial Comparison of Gridded Tmy, Tdy, and Tgy Data Sets*; National Renewable Energy Laboratory (NREL), Golden, CO., 2014;
53. Fanego, V.L.; Rubio, J.P.; Peruchena, C.M.F.; Romeo, M.G.; Tejera, S.M.; Santigosa, L.R.; Balderrama, R.X.V.; Tirado, L.F.Z.; Pantaleón, D.B.; Pérez, M.S.; et al. A novel procedure for generating solar irradiance TSYs. *AIP Conf. Proc.* **2017**, *1850*, 140015, doi:10.1063/1.4984523.
54. Kneifel, J.; O'Rear, E. An Assessment of Typical Weather Year Data Impacts vs. Multi-year Weather Data on Net-Zero Energy Building Simulations. *NIST Spec. Publ.* **2016**, *1204*.
55. Westney, R. Assessing the risk in capital-intensive opportunities. *Oil Gas Financ. J.* **2011**.
56. Pecenak, Z.K.; Stadler, M.; Fahy, K. Efficient multi-year economic energy planning in microgrids. *Appl. Energy* **2019**, *255*, 113771, doi:10.1016/j.apenergy.2019.113771.
57. Lee, B.D.; Sun, Y.; Hu, H.; Augenbroe, G.; Paredis, C.J.J. A FRAMEWORK FOR GENERATING STOCHASTIC METEOROLOGICAL YEARS FOR RISK-CONSCIOUS DESIGN OF BUILDINGS. *Proc. SimBuild* **2012**, *5*, 345-352–352.
58. Hirth, L.; Steckel, J.C. The role of capital costs in decarbonizing the electricity sector. *Environ. Res. Lett.* **2016**, *11*, 114010.
59. Helton, J.C. *Conceptual and computational basis for the quantification of margins and uncertainty*; Sandia National Laboratories (United States). Funding organisation: US Department of Energy (United States), 2009;
60. Swiler, L.P.; Paez, T.L.; Mayes, A.L. Epistemic uncertainty quantification tutorial. In Proceedings of the In Proceedings of the IMAC XXVII conference and exposition on structural dynamics, number 294; 2009.
61. Tian, W.; Heo, Y.; de Wilde, P.; Li, Z.; Yan, D.; Park, C.S.; Feng, X.; Augenbroe, G. A review of uncertainty analysis in

building energy assessment. *Renew. Sustain. Energy Rev.* **2018**, *93*, 285–301, doi:10.1016/j.rser.2018.05.029.

62. Nielsen, K.; Blanc, P.; Vignola, F.; Ramírez, L.; Blanco, M.; Meyer, R. *Meteorological Data Sets for CSP/STE Performance Simulations – Discussion of current practices*; SolarPACES Report; 2016;
63. Dorf, R.C. *The technology management handbook*; CRC Press, 1998; ISBN 1-4200-5056-7.
64. Heller, P. *The Performance of Concentrated Solar Power (CSP) Systems: Analysis, Measurement and Assessment*; Woodhead Publishing, 2017;
65. Fernández-Peruchena, C.M.; Vignola, F.; Gastón, M.; Lara-Fanego, V.; Ramírez, L.; Zarzalejo, L.; Silva, M.; Pavón, M.; Moreno, S.; Bermejo, D.; et al. Probabilistic assessment of concentrated solar power plants yield: The EVA methodology. *Renew. Sustain. Energy Rev.* **2018**, *91*, 802–811, doi:10.1016/j.rser.2018.03.018.
66. Cebecauer, T.; Suri, M. Typical Meteorological Year Data: SolarGIS Approach. *Energy Procedia* **2015**, *69*, 1958–1969, doi:10.1016/j.egypro.2015.03.195.
67. Espinar, B.; Blanc, P.; Wald, L. *TMY for production*; Project ENDORSE; ARMINES, 2012;
68. CTN 206/SC 117 - CENTRALES TERMOSOLARES UNE 206011:2014. Centrales termosolares. Procedimiento de generación de Año Solar Representativo. 2014.
69. Eck, M.; Kretschmann, D.; Feldhoff, J.F.; Wittmann, M. Considering Uncertainties in Research by Probabilistic Modeling.; American Society of Mechanical Engineers Digital Collection, 2013; pp. 263–271.
70. Larrañeta, M.; Fernandez-Peruchena, C.; Silva-Pérez, M.A.; Lillo-bravo, I.; Grantham, A.; Boland, J. Generation of synthetic solar datasets for risk analysis. *Sol. Energy* **2019**, *187*, 212–225, doi:10.1016/j.solener.2019.05.042.
71. HOMER - Hybrid Renewable and Distributed Generation System Design Software Available online: https://www.homerenergy.com/index.html (accessed on Apr 3, 2020).
72. Aziz, A.S.; Tajuddin, M.F.N.; Adzman, M.R.; Ramli, M.A.M. Feasibility Analysis of PV/Diesel/Battery Hybrid Energy System Using Multi-year Module. *Int. J. Renew. Energy Res. IJRER* **2018**, *8*, 1980–1993.
73. Ramadesigan, V.; Northrop, P.W.C.; De, S.; Santhanagopalan, S.; Braatz, R.D.; Subramanian, V.R. Modeling and Simulation of Lithium-Ion Batteries from a Systems Engineering Perspective. *J. Electrochem. Soc.* **2012**, *159*, R31, doi:10.1149/2.018203jes.
74. Owusu, P.A.; Asumadu-Sarkodie, S. A review of renewable energy sources, sustainability issues and climate change mitigation. *Cogent Eng.* **2016**, *3*, 1167990, doi:10.1080/23311916.2016.1167990.
75. Building Performance Simulation for Design and Operation Available online: https://www.crcpress.com/Building-Performance-Simulation-for-Design-and-Operation/Hensen-Lamberts/p/book/9781138392199 (accessed on Jan 15, 2020).
76. Peruchena, C.F.; Larrañeta, M.; Blanco, M.; Bernardos, A. High frequency generation of coupled GHI and DNI based on clustered Dynamic Paths. *Sol. Energy* **2018**, *159*, 453–457, doi:10.1016/j.solener.2017.11.024.
77. Frimane, Â.; Soubdhan, T.; Bright, J.M.; Aggour, M. Nonparametric Bayesian-based recognition of solar irradiance conditions: Application to the generation of high temporal resolution synthetic solar irradiance data. *Sol. Energy* **2019**, *182*, 462–479, doi:10.1016/j.solener.2019.02.052.
78. Lohmann, S.; Schillings, C.; Mayer, B.; Meyer, R. Long-term variability of solar direct and global radiation derived from ISCCP data and comparison with reanalysis data. *Sol. Energy* **2006**, *80*, 1390–1401, doi:10.1016/j.solener.2006.03.004.
79. Castillejo-Cuberos, A.; Escobar, R. Understanding solar resource variability: An in-depth analysis, using Chile as a case of study. *Renew. Sustain. Energy Rev.* **2020**, *120*, 109664, doi:10.1016/j.rser.2019.109664.
80. Feng, Y.; Chen, D.; Zhao, X. Estimated long-term variability of direct and diffuse solar radiation in North China during 1959–2016. *Theor. Appl. Climatol.* **2019**, *137*, 153–163, doi:10.1007/s00704-018-2579-1.

81. Kershaw, T.; Eames, M.; Coley, D. Comparison of multi-year and reference year building simulations. *Build. Serv. Eng. Res. Technol.* **2010**, *31*, 357–369, doi:10.1177/0143624410374689.
82. Hong, T.; Chang, W.-K.; Lin, H.-W. A fresh look at weather impact on peak electricity demand and energy use of buildings using 30-year actual weather data. *Appl. Energy* **2013**, *111*, 333–350, doi:10.1016/j.apenergy.2013.05.019.
83. Calleja Rodríguez, G.; Carrillo Andrés, A.; Domínguez Muñoz, F.; Cejudo López, J.M.; Zhang, Y. Uncertainties and sensitivity analysis in building energy simulation using macroparameters. *Energy Build.* **2013**, *67*, 79–87, doi:10.1016/j.enbuild.2013.08.009.
84. Comparison of heating and cooling energy simulation using multi-years and typical weather data in South Korea - Hochun Yoo, Kwanho Lee, Geoffrey J Levermore, 2015 Available online: https://journals.sagepub.com/doi/abs/10.1177/0143624414537507 (accessed on Apr 3, 2020).
85. Sun, Y.; Gu, L.; Wu, C.F.J.; Augenbroe, G. Exploring HVAC system sizing under uncertainty. *Energy Build.* **2014**, *81*, 243–252, doi:10.1016/j.enbuild.2014.06.026.
86. Environmental Modelling: An Uncertain Future? Available online: https://www.crcpress.com/Environmental-Modelling-An-Uncertain-Future/Beven/p/book/9780415457590 (accessed on Apr 3, 2020).
87. Macdonald, I.; Strachan, P. Practical application of uncertainty analysis. *Energy Build.* **2001**, *33*, 219–227, doi:10.1016/S0378-7788(00)00085-2.
88. de Wit, S.; Augenbroe, G. Analysis of uncertainty in building design evaluations and its implications. *Energy Build.* **2002**, *34*, 951–958, doi:10.1016/S0378-7788(02)00070-1.
89. Struck, C.; P. J.C.J. Wilde, D.; Evers, J.E.J.; Hensen, J.L.M.; Plokker, W. On selecting weather data sets to estimate a building design's robustness to climate variations. In Proceedings of the 11th IBPSA Building Simulation Conference, 27-30 July; International Building Performance Simulation Association (IBPSA), 2009; pp. 513–520.
90. Braun, M.R.; Altan, H.; Beck, S.B.M. Using regression analysis to predict the future energy consumption of a supermarket in the UK. *Appl. Energy* **2014**, *130*, 305–313, doi:10.1016/j.apenergy.2014.05.062.
91. Du, H.; Underwood, C.; Edge, J. Generating design reference years from the UKCP09 projections and their application to future air-conditioning loads. *Build. Serv. Eng. Res. Technol.* **2012**, *33*, 63–79, doi:10.1177/0143624411431775.
92. Andasol-3 | Concentrating Solar Power Projects Available online: https://solarpaces.nrel.gov/andasol-3 (accessed on Apr 10, 2020).
93. Ohmura, A.; Gilgen, H.; Hegner, H.; Müller, G.; Wild, M.; Dutton, E.G.; Forgan, B.; Fröhlich, C.; Philipona, R.; Heimo, A.; et al. Baseline Surface Radiation Network (BSRN/WCRP): New Precision Radiometry for Climate Research. *Bull. Am. Meteorol. Soc.* **1998**, *79*, 2115–2136, doi:10.1175/1520-0477(1998)079<2115:BSRNBW>2.0.CO;2.
94. Moreno-Tejera, S.; Silva-Pérez, M.A.; Lillo-Bravo, I.; Ramírez-Santigosa, L. Solar resource assessment in Seville, Spain. Statistical characterisation of solar radiation at different time resolutions. Sol. Energy 2016, 132, 430–441.
95. Fernández-Peruchena, C.M.; Polo, J.; Martín, L.; Mazorra, L. Site-Adaptation of Modeled Solar Radiation Data: The SiteAdapt Procedure. Remote Sens. 2020, 12, 2127, doi:10.3390/rs12132127.
96. Polo, J.; Fernández-Peruchena, C.; Salamalikis, V.; Mazorra-Aguiar, L.; Turpin, M.; Martín-Pomares, L.; Kazantzidis, A.; Blanc, P.; Remund, J. Benchmarking on improvement and site-adaptation techniques for modeled solar radiation datasets. *Sol. Energy* **2020**, *201*, 469–479, doi:10.1016/j.solener.2020.03.040.
97. CTN 206/SC 117 - CENTRALES TERMOSOLARES UNE 206013:2017. Centrales termosolares. Procedimiento de generación de años percentiles de radiación solar. 2017.
98. Yang, D.; Bright, J.M. Worldwide validation of 8 satellite-derived and reanalysis solar radiation products: A preliminary evaluation and overall metrics for hourly data over 27 years. *Sol. Energy* **2020**, doi:10.1016/j.solener.2020.04.016.